Pulsed Plasma-Enhanced Chemical Vapor Deposition from Hexafluoropropylene Oxide: Film Composition Study

SCOTT J. LIMB,[1] DAVID J. EDELL,[2] EDWARD F. GLEASON,[3] KAREN K. GLEASON[1]

[1] Department of Chemical Engineering, MIT, Cambridge, Massachusetts 02139

[2] Division of Health and Sciences, Harvard University, Cambridge, Massachusetts 02139

[3] MIT Lincoln Laboratory, Lexington, Massachusetts 02173

Received 4 June 1997; accepted 9 August 1997

ABSTRACT: Films deposited using pulsed plasma-enhanced chemical vapor deposition (PECVD) from hexafluoropropylene oxide (HFPO) were investigated by X-ray photoelectron spectroscopy (XPS). As compared to continuous rf PECVD, pulsed excitation increases the CF_2 fraction in the film. Film composition was determined as a function of plasma processing conditions including on-time, off-time, pressure, flow rate, substrate temperature, electrode spacing, substrate potential, and input power. Varying the on–off pulsing cycle resulted in compositional control of the deposited films. At a low duty cycle $[t_{on}/(t_{on} + t_{off})]$, up to 70% CF_2 could be incorporated into the film. The input gas, HFPO, may facilitate greater CF_2 incorporation into the films as this gas thermally decomposes into a difluorocarbene. Both absolute on-time and off-time, rather than simply duty cycle, are important parameters for determining film composition. A simple model was developed to describe the experimentally determined variation $\%CF_2$ as a function of substrate temperature and off-time. This model accounts for changes in film composition due to plasma-surface modification and differences in gas-phase chemistry. The model suggests that surface modification by the plasma is the dominant factor only for long on-times or for low deposition rates. However, the gas-phase concentration of CF_2 relative to other film-forming species is typically the controlling factor under conditions which achieve the high $\%CF_2$ in the film. The gas-phase composition will depend on both abslute on-time and off-time, rather than simply on the duty cycle. © 1998 John Wiley & Sons, Inc. J Appl Polym Sci **67:** 1489–1502, 1998

INTRODUCTION

Fluorocarbon plasma-enhanced chemical vapor deposition (PECVD) has been investigated as a possible means of depositing films similar in composition to bulk polytetrafluoroethylene [PTFE, $(CF_2)_n$, Teflon™]. Bulk Teflon has many remarkable properties, including a low dielectric constant of 2.1,[1] low coefficient of friction between 0.05 and 0.08,[2] low permeability constant,[2] and biocompatibility.[3–5] The electrical properties of bulk PTFE makes it an excellent candidate for an interlayer dielectric. Also, the known biocompatibility of bulk Teflon suggests that these coatings could be used in a variety of biomedical applications including lead wires for pacemakers, catheter inserts, neural probes, and implantable tubing. Furthermore, PECVD films can be pinhole-free, conformal, excellent permeation barriers, sterile upon deposition, and deposited onto a variety of

Correspondence to: K. K. Gleason.
Contract grant sponsor: NIH; contract grant number: NO1-NS-3-2301.

Journal of Applied Polymer Science, Vol. 67, 1489–1502 (1998)
© 1998 John Wiley & Sons, Inc. CCC 0021-8995/98/081489-14

different substrates.[6] Thus, this motivates the desire to make PECVD films similar in properties and composition to bulk PTFE.

There are many studies detailing the extensive research into the PECVD of fluorocarbon thin films.[7–10] Most used continuous radio-frequency (rf) PECVD within the glow region and resulted in PECVD films differing in composition from that of bulk PTFE. A typical fluorine-to-carbon (F/C) ratio for films deposited under these various process conditions is only ~ 1.6. Films with high CF_2 fractions downstream from the glow discharge have been deposited, but deposition rates were low.[11,12] Also, in the presence of H_2, variable power studies of C_2F_6 plasma have deposited materials ranging in CF_2 content from 53 to 8%.[13,14] At the early stage of growth (i.e., after one short rf pulse), the deposited film contained nearly 100% CF_2 species. From this work, high CF_2 content could be achieved via single-pulsed deposition.

Films with up to 80% CF_2 have been made using pulsed PECVD from hexafluoropropylene oxide (HFPO)[15–17] as a precursor. Pulsed PECVD gave similar results for deposition from CF_4 and C_2F_6 gases with H_2 addition.[18] By increasing the CF_2 content, flexible rather than brittle wire coatings from HFPO were made by pulsed PECVD.[16] For these depositions, the applied power is pulsed on for ~ 10 ms rather than being continuously applied. Studies depositing fluorocarbons using short pulses (<1 ms) have also been investigated.[19] During the pulse, the substrate is exposed to the glow discharge which is composed of ions, electrons, excited species, and neutrals. In the off-time between the pulses, the long-lived neutral intermediates dominate.[20] The pulsing process is related to remote or afterglow PECVD,[21] where the substrates are placed outside the glow region. Although both pulsed and downstream PECVD allow long-lived neutral intermediates to be involved in the deposition process, only the pulsed PECVD allows for ion bombardment of the substrate. The transport of the reactive gas-phase species to the growth surface is simpler for pulsed PECVD than for the downstream configuration. In addition, pulsed rf discharges have been used to study the plasma kinetics as the dynamic process gives direct information on the rates of chemical and physical phenomena in the plasma.[20] Control of film properties and deposition rates,[22] uniformity,[23] and etching[24] have also been investigated by power modulation.

Carbon 1*s* X-ray photoelectron spectroscopy (C1*s* XPS) has been widely used to determine the composition of fluorocarbon PECVD films.[7,8] In addition to CF_2 groups, comparable concentrations of CF_3, CF, and quaternary carbon moieties ($\underline{C}$—CF and carbon with no β-substituted fluorine) were also found.[7,8] The CF and quaternary carbon groups are potential crosslinking sites within the polymeric film. Reducing crosslinking is critical in achieving flexible coatings.[16] Unlike bulk PTFE, continuous PECVD films may contain carbon–carbon double bonds.[25,26] The binding energy assigned to the different carbon environments for CF_3, CF_2, CF, $\underline{C}$—CF, and carbon with β-substituted fluorine are 294, 292.1, 289.5, and 287.3, and 285.0 eV, respectively.[8] Since XPS is a surface analytical tool, depth characterization is achieved between 5 and 50 Å (ref. 27) and, thus, the peak at 285.0 may contain contributions from extraneous carbon. Furthermore, charging effects usually shift the binding energies and need to be accounted for.

In this article, an extensive study of film compositions of pulsed PECVD films deposited from HFPO are reported. The goal was to better understand the conditions at which high CF_2 fraction films can be deposited. Composition as a function of on-time, off-time, pressure, flow rate, substrate temperature, input power, electrode spacing, and input power were examined. Furthermore, a simple model for CF_2 film fraction as a function of substrate temperature and off-time was developed and compared with the data.

BACKGROUND

In this article, only the film's composition will be discussed as a function of process conditions. The experimentally measured deposition rates as a function of processing conditions have been previously reported and modeled.[17] Furthermore, discussions for the gas-phase plasma chemistry and surface modification were also reported.[17] In that work, the fluorocarbon plasma chemistry occurring during the plasma on-time were grouped into the following reactions:

$$\text{HFPO} \rightarrow CF_2 + \text{aldehyde} \quad (1)$$
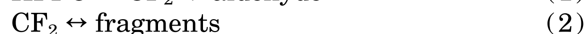
$$CF_2 \leftrightarrow \text{fragments} \quad (2)$$

$$\text{aldehyde} \rightarrow \text{fragments} \quad (3)$$

$$\text{HFPO} \rightarrow \text{fragments} \quad (4)$$

Reaction 1 has been observed via thermal and

Table I Standard Process Conditions

Process Conditions	Default Value	Other Values
Input gas	Hexafluoropropylene oxide (HFPO)	—
Flow rate	23 sccm	5.1 and 12.5 sccm
Pressure	1000 mtorr	400, 750, and 1200 mtorr
Substrate temperature	20°C	−38 to +123°C
On-time	10 ms	2–150 ms
Off-time	400 ms	2–2000 ms
Peak rf power for pulsed PECVD	280 W	140 W
Rf power continous PECVD	50 W	25, 140, 280 W
Substrate potential	Grounded	Isolated
Electrode spacing	1.0 in.	0.5 in.

plasma excitation as a primary decomposition pathway for HFPO at low pressure.[28] Recently, our group has shown that this same mechanism can explain the activation energy observed for pyrolytic CVD from HFPO.[29] We hypothesize that this pathway is also important for pulsed PECVD. In support of this idea, the observed low oxygen content of the pulsed PECVD films is consistent with the majority of the oxygen leaving the reactor in the form of the aldehyde or the likely decomposition products of reaction 3: CO and COF. In addition, the production and subsequent polymerization of difluorocarbene (CF_2) would incorporate CF_2 units into the film.

With HFPO, two factors are anticipated to be important for depositing films with high CF_2 percentages. First, the gas-phase mol fraction of CF_2 relative to other film-forming fluorocarbon species, CF_3 and CF, must be high. Thus, reactions 2, 3, and 4 must be minimized. Second, once deposited, CF_2 groups in the film must be protected form further surface reactions initiated by energetic bombardment and chemical etching.

Pulsed plasma excitation could affect the gas-phase composition in the reactor, the ion bombardment of the growing surface, or both. Undesired processes, such as eqs. (2) and (3), which create gaseous precursors other than difluorocarbene, are more likely the greater the number of pulsed excitation periods a gas-phase molecule experiences before flowing out of the reaction zone. Thus, the relationship of the total cycle time, ($t_{on} + t_{off}$), to the residence time of the reaction is important. In addition, varying the duty cycle [$t_{on}/(t_{on} + t_{off})$] will alter the exposure of depositing material to the glow discharge, especially to the effect of ion bombardment. Indeed, it was observed that deposition rates were a function of both the total cycle time and the duty cycle.[17] Thus, deposition using plasma excitation for t_{on} (ms) followed by no excitation for t_{off} (ms) will be referred to as t_{on}/t_{off} films.

EXPERIMENTAL

Plasma Reactor and Operating Conditions

A parallel-plate stainless-steel plasma reactor was used in this work and was described in detail previously.[17] The powered electrode (11.4-cm-diameter aluminum disk) and grounded electrode (11.4-cm-diameter aluminum cylinder) are spaced 1 in. apart with samples placed on the grounded electrode. The total reactor volume, excluding the electrode volume, is 5100 cm^3. The effective volume in between the two electrodes is 261 cm^3. Test grade, 1–50 Ω cm, n-type, (100) 4-in.-diameter, silicon wafers were used as substrates, having a thickness in the range of 475–575 μm. Undiluted HFPO (from PCR Inc., 99% purity) was used as the CVD precursor. Unless otherwise stated, these silicon wafer substrates were placed on the bottom grounded electrode. In some cases, silicon wafers were electrically isolated by placing them on $\frac{1}{4}$-in.-thick glass plates of the same areal dimension.

Reactor pressures of 1.2, 1.0, 0.75, and 0.40 Torr were used along with HFPO flow rates of 23, 12.5, and 5.1 sccm (STP). The rf power source (13.56 MHz) was pulsed by varying on-times from 2 to 150 ms and off-times from 10 to 2000 ms. When continuous rf excitation was used, the power was set at 280, 140, 50, or 25 W. For all but one pulsed PECVD experiment, the peak power was fixed at 280 W. Unless otherwise noted,

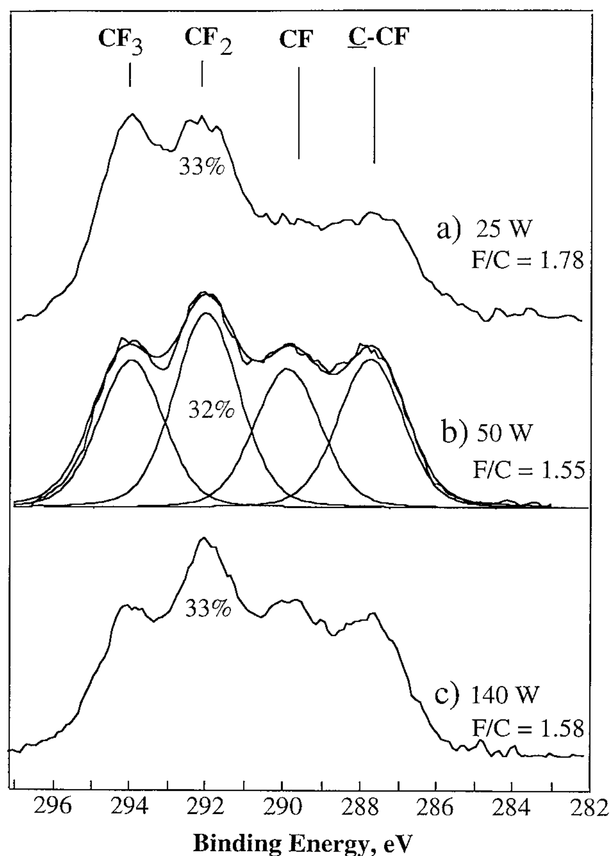

Figure 1 C1*s* XPS spectra of continuous PECVD films deposited using (a) 25, (b) 50, and (c) 140 W of input rf power. No film was deposited at 280 W of input rf power. These experiments employed a flow rate of 12.5 sccm while all other process parameters were held fixed at their default value (Table I). The four deconvoluted components are explicitly shown in (b), representing, in order of decreasing binding energy, —CF_3, —CF_2, —CF, and quaternary carbon. For all films, results of the deconvolution yielded the %CF_2 and F/C ratio, as shown. Note the relatively small variation in %CF_2 which results from changing the input power to the continuous PECVD process.

the substrate temperature was maintained with the grounded electrode at 293 ± 3 K with backside water cooling. Experiments at substrate temperatures ranging from 235 to 396 K were performed either by cooling the grounded electrode with cold nitrogen gas or by resistively heating an electrically grounded aluminum plate on the grounded electrode.

Film Characterization

XPS was performed on a Perkin-Elmer 5100 spectrometer employing a monochromatic $MgK\alpha_{1,2}$ exciting radiation source. The Mg anode X-ray source was operated at 300 W with a pass energy of 17.9 eV for the carbon 1*s* (C1*s*) spectra and a pass energy of 178.95 eV for the survey scans. The angle between the X-ray source and the analyzer was set at 45°. Charging effects of up to 3 eV were corrected by comparing the F/C ratios obtained by the survey scans to those calculated from the C1*s* spectra. The samples were not sensitive to X-ray damage as minimal changes were seen after 45 min of exposure. Only a 10-min exposure was required to obtain the C1*s* spectra. For reference, C1*s* spectra were also taken of a bulk PTFE sample. Finally, features at 285.0 eV representing either extraneous carbon or carbon from the plasma were visibly absent or minimal in all of the spectra shown in this article.

Deconvolution of the XPS line shapes was performed using the Perkin-Elmer 5100 software which incorporates an intensive volume of background data for binding energies. Good correlation between the predicted and experimental spectra was gathered assuming 60/40 Gaussian/Lorentzian line shapes with the full-width at half-maximum of each line shape set at 2 eV. Also, the central binding energies were allowed to vary ±0.2 eV for the CF_3, CF, and $\underline{C}$—CF components while keeping CF_2 fixed. The estimated standard deviation of the deconvolution is ±2% %CF_x. Since adhesion is a significant concern for fluorocarbon films, a tape test was performed on one hundred 1- × 1-mm squares scored into selected films using a razor. On this basis, reasonable adhesion was observed, showing no failure on any of the squares tested.

RESULTS AND DISCUSSION

Effect of Power on Continuous PECVD

Unless otherwise noted, the reactor conditions used appear in Table I. In Figure 1, carbon 1*s* (C1*s*) XPS spectra for continuous PECVD at 12.5 sccm using three different power levels are shown. Deconvolution shows features assigned as CF_3 (294 eV), CF_2 (292 eV), CF (289.5 eV), and $\underline{C}$—CF (287.3 eV).[8] Integration of the CF_3, CF_2, CF, and $\underline{C}$—CF components allows a F/C ratio to be calculated from the C1*s* spectra. F/C ratios of 1.78, 1.55, and 1.58 were found for the PECVD films deposited at 23, 50, and 140 W, respectively.

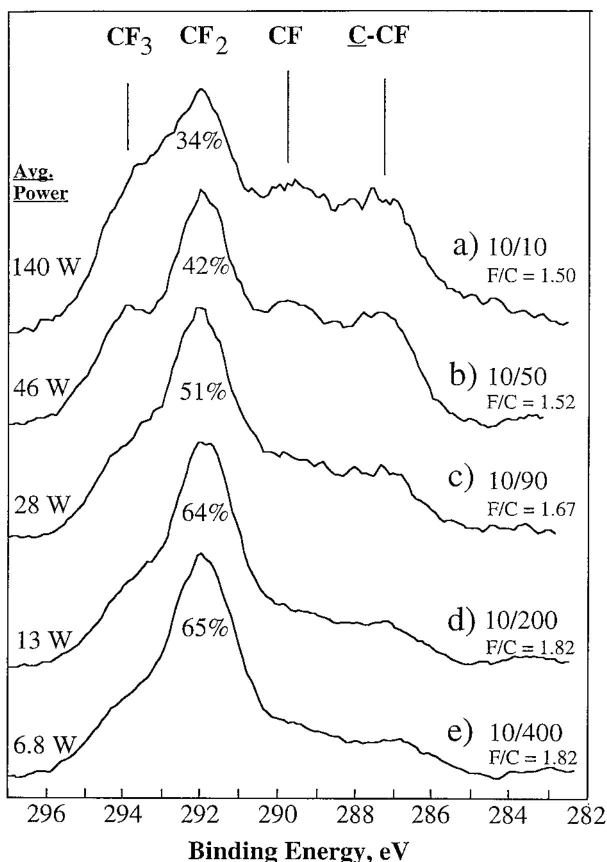

Figure 2 C1*s* XPS spectra of pulsed PECVD films deposited using 10 ms of on-time followed by off-times of (a) 10, (b) 50, (c) 90, (d) 200, and (e) 400 ms. All other process parameters were held fixed at their default values (see Table I). Deconvolution results show a significant monotonic increase in both $\%CF_2$ and the F/C ratio as off-time increases. To facilitate comparison to Figure 1, the average power of each pulse condition was calculated by multiplying the peak power (280 W) by the duty cycle. Continuous and pulsed PECVD films deposited at similar average powers can differ significantly in composition. Specifically, compare Figure 1(a) (25 W) to Figure 2(c) (28 W).

The F/C ratios calculated from the C1*s* spectra agree to within 5% of the values measured by XPS survey scans.

Figure 1 shows that only relatively small changes in CF_2 composition result from varying the peak power for continuous PECVD. No statistically significant difference exists between the C1*s* XPS spectra for the 50 and 140 W depositions. At 25 W, the $\%CF_3$ increases relative to the %CF and %CF—CF. However, the $\%CF_2$ for the 25 W deposition, 33%, is similar to that for the films grown at higher powers. Continuous PECVD was also attempted at 280 W. However, no deposition resulted. Indeed, fluorocarbon films placed in the reactor under these conditions were etched.

The continuous PECVD results will be compared to those for pulsed PECVD. In all cases except one, the peak power for the pulsed PECVD will be set at 280 W. As noted above, at this power setting, continuous PECVD does not occur. The average power for pulsed PECVD will be changed by varying the duty cycle $[t_{on}/(t_{on} + t_{off})]$ at a fixed peak power.

The percentages of CF_3, CF, and C—CF in Figure 1 for the 50 and 140 W spectra are comparable. The same is true for the majority of the spectra in this work. The CF_2 fraction is also an important figure of merit for the films relative to bulk PTFE (100% CF_2). For all the films in this study, XPS survey scans show that the oxygen content is less than 2 atomic %. This indicates that little oxygen from the HFPO precursor is being incorporated into the film. In addition, some or all of the incorporated oxygen impurities may result from atmospheric exposure.

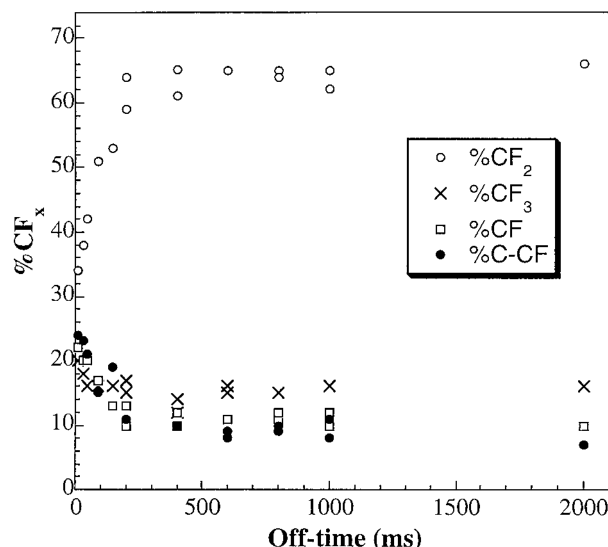

Figure 3 The composition, as determined from deconvolution of the C1*s* XPS spectra, of pulsed PECVD films deposited using 10 ms of on-time as a function of off-time. Default values (Table I) were used for the other process conditions. The $\%CF_2$ increases with off-time at the expense of the $\%CF_3$, %CF, and % quaternary carbon until a plateau of 66% CF_2 is reached at a long off-time.

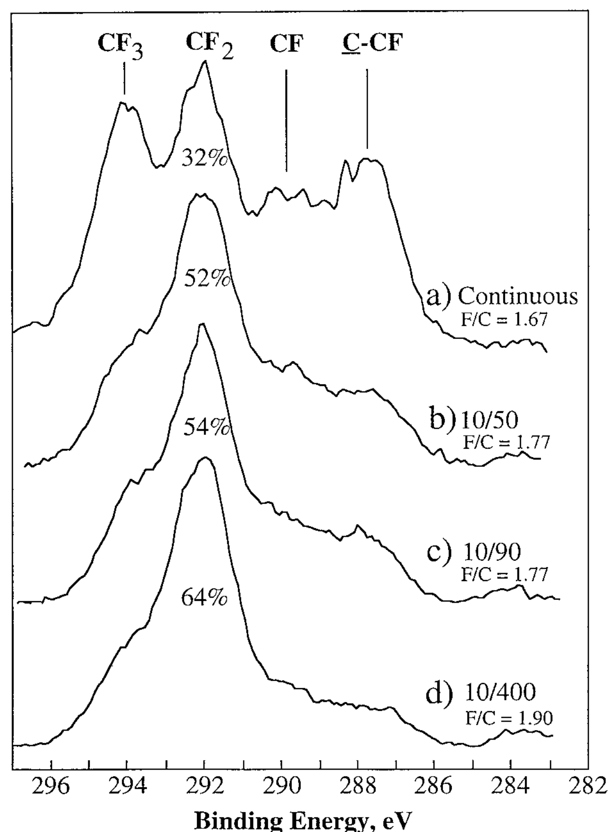

Figure 4 The C1*s* XPS spectra for films deposited onto an electrically isolated substrate. The top spectra (a) are for a continuous PECVD films. The remaining spectra are for pulsed PECVD films using 10 ms on-time with (b) 50, (c) 90, and (d) 400 ms of off-time. A flow rate of 12.5 sccm was employed for all films. All other process parameters were held fixed at their default values (Table I).

Off-Time

Pulsing the rf excitation for 10 ms on followed by 400 ms off (10/400) resulted in a film with 65% CF_2 [Fig. 2(e)], which is substantially higher than the 32% for traditional PECVD deposited at 50 W peak power [Fig. 1(b)]. For the 10/400 pulsed PECVD film [Fig. 2(e)], the F/C ratio is 1.82. As off-time is increased, the CF_2 peak increases while the other peaks representing CF_3, CF, and $\underline{C}$—CF decrease. Results from spectral deconvolution as a function of t_{off} are plotted in Figure 3 with $\%CF_x$ representing $\%CF_3$, $\%CF_2$, %CF, and %$\underline{C}$—CF. The $\%CF_2$ increases with increasing t_{off} until a plateau value of 66% is reached. Likewise, $\%CF_3$, %CF, and %$\underline{C}$—CF decrease with increasing t_{off} until it levels off. Increasing t_{off} from 400 to 2000 ms results in a minimal change of $\%CF_2$. For t_{off} greater than 100 ms, the films had more CF_3 than either CF or the $\underline{C}$—CF species, while the opposite was true for shorter off-times. Furthermore, F/C ratios decreased from 1.90 to 1.50 as t_{off} decreased from 2000 to 10 ms. Reducing the input power from 280 to 140 W for a 10/400 on-off setting did not affect the composition of the film. The deconvoluted XPS spectra at 140 W gave 63% CF_2, 18% CF_3, 10% CF, and 8% $\underline{C}$—CF, corresponding to a F/C ratio of 1.90.

Comparing Figures 1 and 2 clearly demonstrates that the effects of pulsing the plasma can not be accounted for simply by considering changes in the average applied power. Increasing t_{off} while holding t_{on} fixed decreases both the fraction of time the gas phase is subjected to plasma excitation and the fraction of time the growing film is exposed to ion bombardment. Reduced plasma excitation of the gas may limit undesirable fragmentation reactions [eqs. (2)–(4)], thus increasing the concentration of CF_2 in the gas phase. Reduced ion bombardment may limit the undesired defluorination reaction of the surface. Both effects could contribute to the observed increase in $\%CF_2$ in the deposited film and F/C ratio.

Substrate Potential

To investigate the effect of reducing the average ion bombardment energy, substrates were placed on an electrically isolated glass plate. Figure 4 shows the resulting C1*s* XPS spectra for a continuous PECVO film at 50 W and for 10/50, 10/90, and 10/400 films at 280 W. Comparing the continuous PECVD spectra at 50 W for the grounded [Fig. 1(b)] and the isolated [Fig. 4(a)], the CF_2 percentages are identical. However, there is slightly less intensity in the defluorinated species, CF and CF_2, for the isolated substrate corresponding to a lower F/C ratio (1.50). The results support the hypothesis that energetic ion bombardment leads to defluorination of the growing surface. In contrast, the 10/400 pulsed PECVD films [Figs. 2(e) and 4(d)] show virtually indistinguishable spectra. Thus, at the low-duty cycle associated with the 10/400 on–off conditions, ion bombardment has a negligible impact on the film composition. Also, the similarity of Figures 2(e)

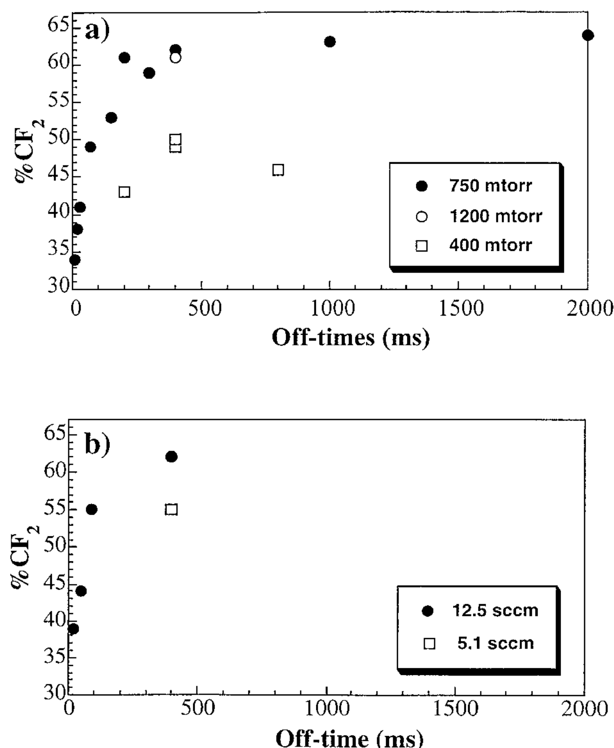

Figure 5 (a) The effect of pressure on the $\%CF_2$ in pulsed PECVD films deposited using 10 ms of on-time as a function of off-time. At 750 and 1200 mtorr, the results are similar to those for 1000 mtorr (Fig. 2), reaching a plateau of approximately 66% CF_2 at long off-time. At 400 mtorr, less CF_2 is incorporated into the film at all measured values of off-times. All other process parameters were held fixed at their default values (Table I). (b) The effect of flow rate on $\%CF_2$ in the pulsed PECVD films at 10 ms on-time and different off-times. The results at 12.5 sccm compare well with the default 23 sccm flow rate (Fig. 3). A lower $\%CF_2$ is observed for the 5.1 sccm flow rate. All other process conditions are as listed in Table I.

and 4(d) confirms that gas-phase chemistry is not significantly perturbed by the addition of the glass plate under the substrate. On the other hand, at the shorter off-times (50 and 90 ms), the fraction of the growing surface exposed to ion bombardment may be significant. The $\%CF_2$ for the 10/50 and 10/90 films are higher for the electrically isolated substrates than for the grounded substrate samples [Fig. 2(b,c)].

Pressure

Figure 5(a) shows that $\%CF_2$ at 750 and 1200 mTorr as function of the off-time are indistinguishable from the results at 1000 mTorr (Fig. 3). However at 400 mTorr, significantly lower $\%CF_2$ was observed. Furthermore, the F/C ratio at 10/400 for the 400 mTorr conditions (F/C = 1.72) decreased compared to the higher pressure data (F/C = 1.82). This indicates that greater gas-phase fragmentation and surface interaction defluorination may be occurring at the lower pressure, resulting in lower $\%CF_2$ in the film. Lowering pressure causes the average electron energy to increase, potentially increasing the rate of fragmentation processes [eqs. (2)–(4)]. This would decrease the gas-phase concentration of CF_2 relative to the other species. Also, longer mean free paths at the lower pressure could increase the energy of ion bombardment and lead to significant surface defluorination.

Flow Rate

In Figure 5(b), $\%CF_2$ as a function of off-time at 12.5 and 5.1 sccm is shown. Again, monotonic increases in $\%CF_2$ as off-time increased were seen at the lower flow rate of 12.5 sccm. At 23 and 12.5 sccm, CF_2 fractions are similar. This change in flow rate did not alter the deposition rate.[17] However, at 400 ms off-time, the 5.1 sccm flow rate results in films with 55% CF_2. The growth rate is also reduced at the lowest flow rate.[17] This lower CF_2 value may result from undesirable fragmentation reactions [eqs. (2)–(4)] occurring to a larger degree when subsequent excitation periods occur before reactive precursors and fragments created by the previous pulse can exit the reactor. Indeed, the residence time is 3.7 s, which is much greater than one pulse cycle ($t_{on} + t_{off}$).

Substrate Temperature

In Figure 6, $\%CF_x$ is plotted as a function of the substrate temperature (T_s) at flow rates of 23 sccm ($T_s \leq 20°C$) and 12.5 sccm ($T_s \geq 20°C$). Because very little difference between these two flows rates were observed in Figure 5(b), data from both 23 and 12.5 sccm runs were combined. The $\%CF_2$ was 62 ± 3% for substrate temperature from −26 to 69°C. A slightly lower value of 55% was measured at 126°C. Furthermore, below 20°C, the F/C ratios were higher than those above. A difference is seen in the relative concentration of CF_3 compared to CF and $\underline{C}$—CF species.

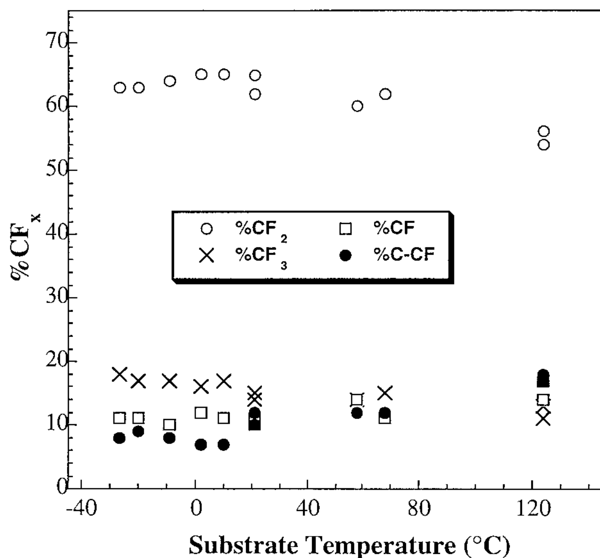

Figure 6 The effect of substrate temperature on the composition of pulsed PECVD films deposited using 10 ms of on-time and 400 ms of off-time. A flow rate of 23 sccm was used below 20°C, while 12.5 sccm was used for the higher-temperature depositions. Only minor variations in composition result from varying the substrate temperature.

Below 20°C, films had higher $\%CF_3$ than either CF or C—CF, 16–18% compared to 7–12%. On the other hand, as substrate temperature increased above 20°C, $\%CF_3$ decreased, eventually having a lower value than either CF or C—CF. At 126°C, the $\%CF_3$ was 12% ± 1%. Overall, relatively small changes in $\%CF_x$ were observed with the substrate temperature change even though the deposition rate changed dramatically. As substrate temperature decreased from 126 to −26°C, the deposition rate increased from 0.4 to 2.6 Å/cycle.[17]

The similarity in $\%CF_2$ suggests, not surprisingly, that gas-phase chemistry is relatively unaffected by substrate temperature. Earlier (Fig. 4), ion bombardment was shown to have minimal effect at a 10/400 on-off setting. The lower $\%CF_2$ at 126°C may indicate that ion-bombardment effects become relatively more important when film growth becomes slow. A low deposition rate results in a higher fraction of film being exposed to ion bombardment. Furthermore, note that films with high CF_2 fractions were deposited at a high substrate temperature. Such films are likely to have improved the thermal stability compared to films deposited at lower substrate temperatures.

On-Time

In Figure 7, $\%CF_x$ is shown as a function of t_{on} while holding the t_{off} constant at 400 ms and flow rate at 12.5 sccm. As t_{on} is increased from 2 to 150 ms, the $\%CF_2$ in the film decreased from 70 to 36% (Fig. 7) and the F/C ratio decreased from 1.94 to 1.62. At short on-times (<10 ms), the $\%CF_3$ is greater than either the %CF or %C—CF. However, at longer on-times, the percentages of all three species become similar. The decrease of $\%CF_3/(\%CF + \%C—CF)$ with increased on-time demonstrates the defluorinating nature of the plasma. Due to the longer on-time, a greater overall fraction of the film may be exposed to the defluorinating conditions. Furthermore, greater fragmentation of gas-phase CF_2 [eq. (2)–(4)] may be occurring as on-time is increased. Both these effects may result in lowering the $\%CF_2$ and increasing the %CF and %C—CF in the films.

Electrode Spacing

In Figure 8, C1*s* spectra are shown for films deposited at an electrode spacing of $\frac{1}{2}$ and 1 in. (both at 12.5 sccm). With a decrease in electrode spacing, the % CF_2 in the deposited film decreased from

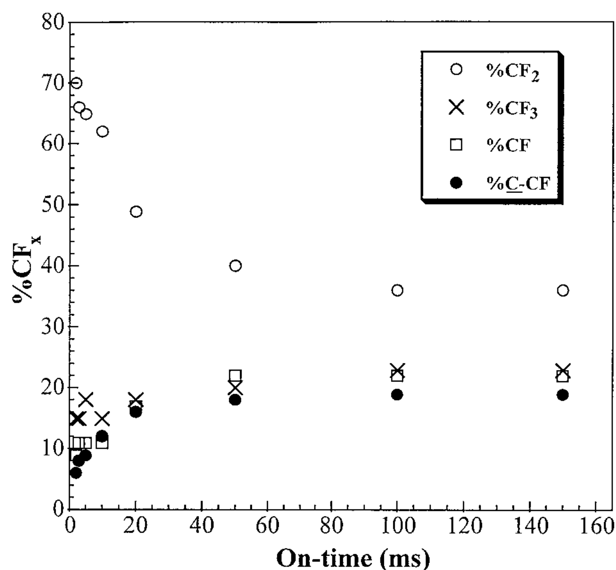

Figure 7 The composition of pulsed PECVD films as a function of on-time holding the off-time fixed at 400 ms. The flow rate was fixed at 12.5 sccm and default values (Table I) were used for the other process conditions. The $\%CF_2$ decreases with on-time until a constant value of 36% is reached.

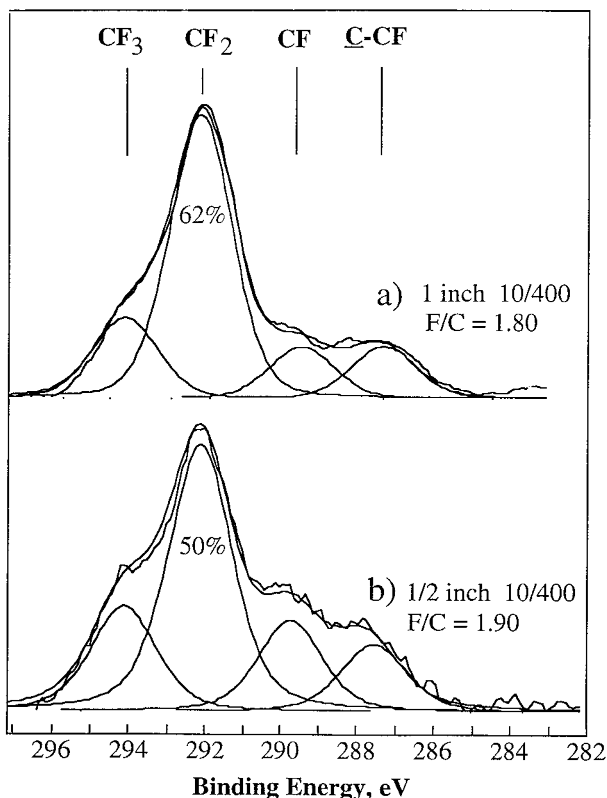

Figure 8 The C1*s* XPS spectra for films deposited at electrode spacings of (a) 1 in. and (b) 0.5 in. For both films, the flow rate used was 12.5 sccm and the other process parameters were fixed at their default values (Table I). The smaller electrode spacing reduced both the $\%CF_2$ and the deposition rate.

62 to 50% for the 10/400 on–off setting. Correspondingly, the deposition per cycle also decreased from 1.8 to 0.97 Å. Two effects may contribute to the lower $\%CF_2$: One is that the lower growth per cycle will result in a larger fraction of the film being exposed to the plasma which increases the undesired defluorination of the surface. The other may be due to the relative concentration of the polymer-forming species changing. Thus, a greater concentration of CF species may be present compared to CF_2.

Ellipsometry

By ellipsometry, the index of refraction ($\lambda = 6328$ Å) was found to be 1.36 ± 0.03 for all pulsed PECVD films in this article. Within experimental error, no definite trends in the refractive index were seen with reactor conditions. A reported value for mostly crystalline PTFE is 1.38 (ref. 30), while for completely amorphous PTFE and its related polymers, refractive indexes of 1.293 ± 0.037 have been calculated.[31] This provides further evidence for the chemical resemblance of pulsed PECVD films to bulk PTFE.

FILM CF_2 FRACTION MODEL

Derivation of Model

Two processes are anticipated to determine the resulting film composition. One is the gas-phase mol fraction of CF_2 relative to other film-forming fluorocarbon species including CF_3 and CF. The gas-phase CF_2 mol fraction depends on plasma chemistry and kinetics. Second, once deposited, CF_2 groups in the film must be protected from further surface reactions initiated by energetic bombardment and chemical etching. Fluorocarbon plasmas produce light, electrons, ions, and reactive neutrals which affect the growing surface. Indeed, ion bombardment,[32] X-ray,[33] electron irradiation,[34] and fluorine atoms[35] are capable of altering the surface of bulk PTFE and lowering the CF_2 fraction. Presumably, similar processes occur during fluorocarbon deposition. Since electrons, fluorine atoms, and ions are short (<1 ms)-lived[36,37] after the plasma is extinguished, surface modification can only occur during the on-time. Thus, the total CF_2 in the film during one pulse cycle is determined by the degree of plasma surface modification during the on-time and gas-phase species present during the off-time and on-time.

Although many possible surface chemical rearrangements and defluorinations exist including chain scissions, fluorine abstraction and recombination, and radical recombination, the $\%CF_2$ results will be analyzed with surface modification following a simple first-order reversible process [eq. (5)]:

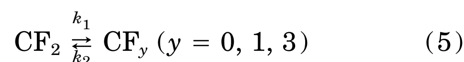

$$CF_2 \underset{k_2}{\overset{k_1}{\rightleftarrows}} CF_y \ (y = 0, 1, 3) \qquad (5)$$

The surface rate constants k_1 and k_2 represent the loss of CF_2 to CF_y (CF_3 or CF or C) and the production of CF_2 from a non-CF_2 moiety, respectively. For simplicity, eq. (5) is intentionally not stoichiometrically balanced. The rate of CF_2 sur-

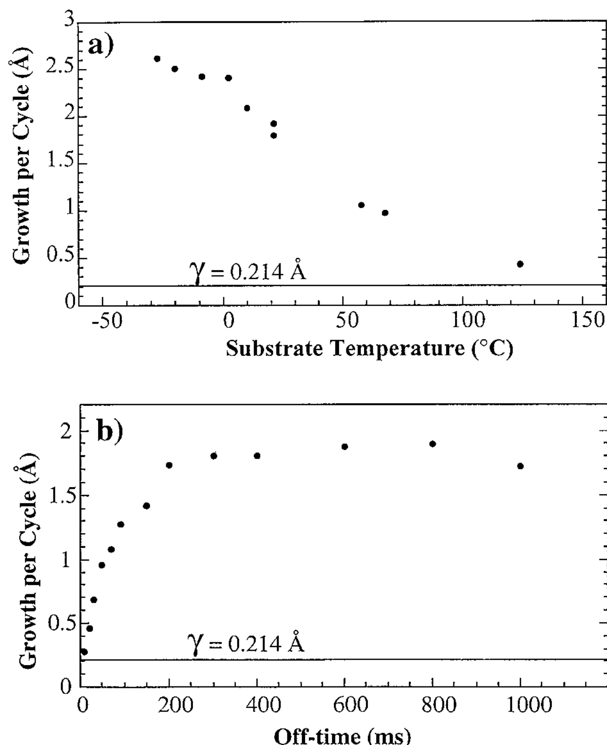

Figure 9 The deposition rate, G, expressed as thickness grown per cycle, as a function of (a) substrate temperature and (b) off-time variation. See Figures 6 and 3, respectively, for more detail on the process conditions. Because the ratio γ/G appears twice in eq. (9), the value γ obtained from nonlinear regression of eq. (9) is also shown.

face modification will be expressed in terms of the surface fractions Θ_2 and Θ_y. The fraction Θ_2 is defined as the total number of CF_2 units over the total number of CF_3, CF_2, CF, and quaternary C units in an effective volume subjected to plasma modification. Also, Θ_y is the fraction of non-CF_2 species in the same effective volume. The depth of the effective volume subjected to plasma modification, X, will be roughly constant at similar plasma conditions. Furthermore, X would represent a depth of at least one monolayer and, due to energetic bombarding species, may comprise several monolayers. Thus, the rate of CF_2 surface modification can be expressed as

$$\frac{d\Theta_2}{dt_{on}} = -k_1\Theta_2 + k_2(1 - \Theta_2) \qquad (6)$$

where $1 - \Theta_2$ is equal to Θ_y.

It is assumed that steady-state concentrations of plasma species which modify the surface are quickly reached. In support of this assumption, ion bombardment is expected to be the major mechanism for surface rearrangement and defluorination. The concentration of ions and electrons will reach a steady state within several hundred microseconds.[36] This time scale is short compared to the typical 10 ms on-time.

Integrating eq. (6) from 0 to t_{on} and Θ_2^0 to Θ_2, the fraction of CF_2 moieties as a function of on-time is

$$\frac{\Theta_2 - \Theta_{ec}}{\Theta_2^0 - \Theta_{eq}} = \exp[-(k_1 + k_2)t_{on}] \qquad (7)$$

where Θ_2^0 is the initial fraction of CF_2 before modification by the plasma and Θ_{eq} is equal to the ratio $[k_2/(k_1 + k_2)]$, which is the equilibrium fraction of CF_2 in the film. Gas-phase plasma kinetics is very complicated with numerous reactions having been proposed to describe the defragmentation and recombination processes in fluorocarbon plasma.[38,39] Furthermore, the steady-state buildup due to incomplete depletion of the CF_x species during shorter off-times adds to the complexity. Experimentally, the lowest %CF_2 composition of the films was 32%. This percentage was observed for continuous plasmas at different input powers (Fig. 1) and also when the substrate was electrically isolated (Fig. 4). Thus, the equilibrium fraction of CF_2, Θ_{eq}, will be set at 0.32 for conditions at 1 torr.

New CF_2 units will be deposited from the gas-phase along with CF and CF_3 species during the on- and off-periods. The new layer will have a thickness, G, and a CF_2 fraction of ϕ_2. At the conditions discussed in this article with a 10 ms on-time, G corresponds to less than a monolayer. In the next cycle, an effective depth of X will again be exposed to plasma modification. Initially, the composition will be ϕ_2 for the top layer of depth G and Θ_2 for the underlying layer of thickness $(X - G)$. Furthermore, it is assumed that G will be less than X because more than one monolayer is probably being affected by the ion bombardment. Thus, the initial fraction of CF_2 in the effective volume for surface modification at $t_{on} = 0$ is

$$\Theta_2^0 = (G/X)\phi_2 + [(X - G)/X]\Theta_2 \qquad (8)$$

The fraction of CF_2 newly deposited from the gas

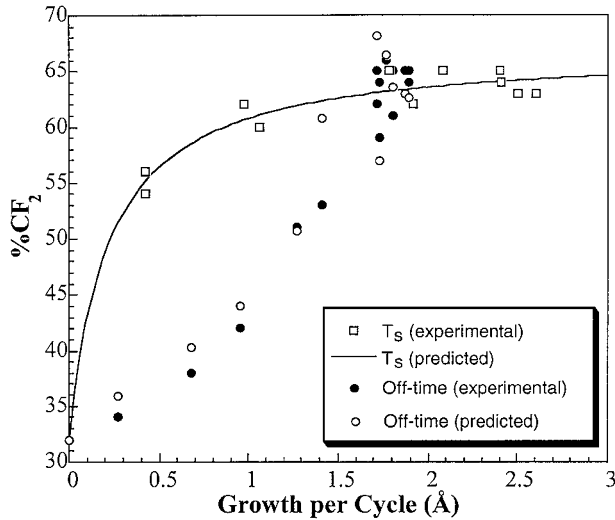

Figure 10 The relationship of $\%CF_2$ in the film to the deposition rate per cycle, G. Experimental data from two sets of films are shown. One (open squares) corresponds to substrate temperature variation, while the other (solid circles) corresponds to off-time variation. See Figures 6 and 3, respectively, for more detail on the process conditions. The model prediction of eq. (9) for substrate temperature variation (solid line) and off-time variation (open circles) are also shown.

phase, ϕ_2, will be dependent on the relative gas-phase concentrations, which is a function of operating conditions mainly on-time, off-time, pressure, and input power.

Using eqs. (7) and (8), the CF_2 fraction measured from C1*s* XPS can be expressed as

$$\Theta_2 = \frac{\frac{\gamma}{G}\Theta_{eq} + \phi_2}{\frac{\gamma}{G} + 1} \tag{9}$$

where γ is

$$\gamma = X\{\exp[(k_1 + k_2)t_{on}] - 1\} \tag{10}$$

The adjustable parameters will be ϕ_2 and γ when on-time and off-time are constant. The parameter, γ, provides a measure of surface modification in terms of depth. At the limit when surface modification is large (i.e., $\gamma \gg G$), Θ_2 will approach Θ_{eq}. This condition can arise when the on-time is long (i.e., continuous plasma) or when deposition is small. When G is much greater than γ, then Θ_2 will approach ϕ_2. Thus, surface modification will be negligible.

Comparison of Data with $\%CF_2$ Model

This section will evaluate the ability of eq. (9) to describe the experimentally measured data. For this comparison, growth per cycle, G, is required. Thus, G is displayed as a function of substrate temperature, T_s, [Fig. 9(a)] and as a function of off-time, t_{off} [Fig. 9(b)]. The corresponding $\%CF_2$ in the films can be found in Figure 6 for variations in T_s and in Figure 3 for variations in t_{off}. In Figure 10, the $\%CF_2$ in the films ($100\ \Theta_2$) is shown as a function of G. The dependence of $\%CF_2$ on G resulting from variations in T_s versus those in t_{off} can be clearly distinguished.

First, the 10/400 pulsed PECVD films deposited at different substrate temperatures will be considered. To perform a nonlinear regression to eq. (9), ϕ_2 and γ will be taken as a constant because both t_{on} and t_{off} are fixed. Furthermore, over this range of temperatures, negligible changes in $(k_1 + k_2)$ will be assumed. Values of $\gamma = 0.214$ Å and $\phi_2 = 0.669$ gave the least-square error. The prediction using these two parameters in eq. (9) is shown as the solid curve in Figure 10. Reasonable correlation between the model and data was obtained ($R^2 = 0.882$). As expected, when G is small relative to γ [vertical line in Fig. 9(a)], Θ_2 approaches $\Theta_{eq} = 0.32$, indicating significant surface modification. For large G, Θ_2 approaches $\phi_2 = 0.669$, indicating that surface modification of the as-deposited surface layer is negligible.

Second, pulsed PECVD films deposited at different off-times will be considered. Figure 10 shows that G alone does not determine the $\%CF_2$ in the films. Since on-time was set at 10 ms, for variations in T_s and t_{off}, γ is expected to be the same and equal to 0.214 Å. However, ϕ_2 may be a function of t_{off} even though t_{on} is constant. The most likely reason for the dependence of ϕ_2 on t_{off} is that CF_3, CF_2, and CF species are loss in heterogeneous reactions which are likely to have different rate constants.[39] Thus, certain species will deposit at a faster rate and contribute more to the film composition when t_{off} is short. At long off-times, this effect is not seen as all the species will have eventually deposited onto the substrate.

The functional dependence of ϕ_2 on t_{off} can be found from the amount of CF_2 as-deposited, which

is the product of ϕ_2 and G. The rate of CF_2 deposition is assumed to be first order in respect to the gas-phase CF_2 since polymer-forming species such as CF_3, CF_2, and CF have been found to deposit with first-order kinetics.[8] Furthermore, a first-order gas-phase loss of CF_2 species was observed and attributed mainly to a first-order heterogeneous surface loss.[20] In a previously developed model for the growth per cycle,[17] an overall single rate constant for the CF_x species was found to accurately describe G. Analogously, the amount of CF_2 as-deposited can be described by

$$\phi_2 G = G_{-}[1 - \exp(-C_2 t_{\mathrm{off}})] \quad (11)$$

where G_{-} is the thickness attributed solely to CF_2 species at long off-times and C_2 is the first-order gas-phase loss constant for CF_2 which includes surface, gas-phase addition, convective losses, and reactor geometry. Equation (11) was derived assuming a negligible net etch or deposition during the on-period and thus all the growth occurs during the off-period.

With eq. (11) and a rearranged form of eq. (9), a nonlinear least-square regression of $[\Theta_2(\gamma + G)]$ as a function of off-time for the data in Figure 3 was performed with G_{-} and C_2 as adjustable parameters. Values of $G_{-} = 1.25$ Å and $C_2 = 0.00857\ \mathrm{ms}^{-1}$ gave the least-square error. The prediction using these two parameters and $\gamma = 0.214$ Å is shown as open circles in Figure 10. Reasonable correlation between the model and data was obtained ($R^2 = 0.885$). Furthermore, from overall growth per cycle modeling, the first-order gas-phase loss constant was $0.0156\ \mathrm{ms}^{-1}$.[17] This overall loss constant is a combination from CF_3, CF_2, and CF gas-phase loss constants. The loss constant for CF_2 is lower than the overall value, which is consistent with CF having a larger loss constant than either CF_2 or CF_3.[20,39]

Sensitivity Analysis

In Table II, the sensitivity of predicted $\%CF_2$ to parameter variations for γ and ϕ_2 was determined for the substrate temperature data (Fig. 10). The value for γ was changed by $\pm 10\%$, while for ϕ_2, it was changed by $\pm 5\%$. The linear coefficient, R^2, and chi square, χ^2, which measure the goodness of fit, were calculated. For variation in γ, small changes in R^2 and χ^2 are seen because surface modification was found to be minimal when the growth per cycle, G, is large. Since most of the data were collected at $G > \gamma$, the data in Figure 10 would not be affected by a $\pm 10\%$ change in γ. On the other hand, variations in ϕ_2 resulted in large changes in the predicted $\%CF_2$ data. This indicates that deposition from the gas phase and the composition of the gas phase are very important in determining the film composition. Only when deposition rates are low and thus the total exposure time are high will the effect of surface interaction be significant.

Table II Sensitivity Analysis

Parameter	R^2	χ^2
No change	.882	16.0
$+\gamma$	.865	18.4
$-\gamma$	.866	18.3
$+\phi_2$	.229	105
$-\phi_2$	.210	108

γ was changed by $\pm 10\%$ and ϕ_2 by $\pm 5\%$. The corresponding goodness of fit is listed and the symbol + or − before each parameter refers to the + or − % change.

CONCLUSIONS

Fluorocarbon composition using pulsed PECVD was controlled over a wide range. Films containing higher $\%CF_2$ were achieved using pulsed PECVD than continuous PECVD. Furthermore, the small observed variations in $\%CF_2$ for the continuous plasma films suggest that an equilibrium surface concentration of CF_2 of approximately 32% is present at 1000 mtorr.

Comparison of the deposition onto grounded and electrically isolated substrates showed that ion bombardment is not a major factor in determining pulsed PECVD film composition at low duty cycles. In addition, the duty cycle alone does not determine film composition. Even though the average power for 10/90 and 50/400 on–off settings is nearly identical, different $\%CF_2$ were measured. Differences in transient gas-phase concentrations may be responsible for these observations. Also, surface modification due to the differences in on-times may contribute to these observations.

A model developed to describe the $\%CF_2$ in the film suggests that surface modification often plays

only a minor role in determining film composition. Surface modification only becomes significant at long on-times and low deposition conditions. The gas-phase concentration of CF_2, which determines the composition of the deposited layer, was found to be the most important in determining the $\%CF_2$ predicted by the model.

Plasma chemistry can be very complex, which makes it difficult to control selectivity. However, since pulsing the plasma excitation varies the degree of ion bombardment, chemical etching of the growing surface and gas-phase reactions, film composition and gas-phase composition can be better controlled. HFPO has a know gas-phase decomposition pathway to difluorocarbene and pulsed excitation may provide a way to favor this reaction pathway over the formation of other decomposition products. Indeed, short on-times resulted in the highest $\%CF_2$ in the film. In addition, shorter off-times lowered the $\%CF_2$ in the film. Thus, subjecting reactant molecules to multiple rf pulses may enhance undesirable fragmentation reactions. To deposit films with a high $\%CF_2$, we speculate that pulse conditions must be selected which result in both a high gas-phase mole fraction of difluorocarbene relative to other film-forming fluorocarbon species such as CF_3 and CF. In addition, once the CF_2 polymerizes on the surface, it must be protected from surface defluorination reactions. This can be achieved by maintaining low on-times with high off-times. The conditions used as default values in this study (Table I) provide a reasonable compromise to achieve high $\%CF_2$ in the film at significant deposition rates, while at the same time avoiding powder formation or nonstable pulsed-plasma conditions.

We wish to gratefully acknowledge the NIH for support of this work under contract NO1-NS-3-2301.

REFERENCES

1. P. Ehrlich, *J. Res. Natl. Std.,* **51,** 185 (1953).
2. S. V. Gangal, in *Encyclopedia of Polymer Science and Engineering,* 2nd ed., H. F. Mark, N. M. Bikales, C. G. Overberger, G. Menges, and J. I. Kroschwitz, Eds., Wiley, New York, 1989, Vol. 16, p. 577.
3. L. A. Thomson, F. C. Law, K. H. James, and N. Rushton, *Biomaterials,* **12,** 781 (1991).
4. R. Guidoin, N. Chakfe, S. Maurel, T. How, M. Batt, M. Marois, and C. Gosselin, *Biomaterials,* **14,** 678 (1993).
5. D. E. Ocumpaugh and H. L. Lee, in *Biomedical Polymers,* A. Rembaum and M. Shen, Eds., Marcel Dekker, New York, 1971, p. 101.
6. B. D. Ratner, A. Chilkoti, and G. P. Lopez, in *Plasma Deposition, Treatment, and Etching of Polymers,* R. d'Agostino, Ed., Academic Press, San Diego, 1990, p. 463.
7. H. Yasuda, *Plasma Polymerization,* Academic Press, Orlando, FL, 1985.
8. R. d'Agostino, F. Cramarossa, F. Fracassis, and F. Illuzzi, in *Plasma Deposition Treatment, and Etching of Polymers,* R. d'Agostino, Ed., Academic Press, San Diego, 1990, pp. 95–162.
9. A. T. Bell, *Top. Curr. Chem.,* **94,** 43 (1980).
10. E. Kay, J. Coburn, and A. Dilks, *Top. Curr. Chem.,* **94,** 1 (1980).
11. D. F. O'Kane and D. W. Rice, *J. Macromol. Sci.-Chem. A,* **10,** 567 (1976).
12. H. Yasuda, *J. Polym. Sci. Macromol. Rev.,* **16,** 199 (1981).
13. R. d'Agostino, F. Cramorossa, F. Fracassi, E. Desimoni, L. Sabbatini, P. G. Zambonin, and G. Caporiccio, *Thin Solid Films,* **143,** 163 (1986).
14. R. d'Agostino, P. Favia, F. Fracassi, and F. Illuzzi, *J. Polym. Sci. Part A Polym. Chem.,* **28,** 3387 (1990).
15. C. R. Savage, R. B. Timmons, and J. W. Lin, *Adv. Chem. Ser.,* **236,** 745 (1993).
16. S. J. Limb, K. K. Gleason, D. J. Edell, and E. F. Gleason, *J. Vac. Sci. Technol.,* to appear.
17. S. J. Limb, D. J. Edell, E. F. Gleason, and K. K. Gleason, to appear.
18. N. M. Mackie, N. F. Dalleska, D. G. Castner, and E. R. Fisher, *Chem. Mater.,* **9,** 349 (1997).
19. H. Yasuda and T. Hsu, *J. Polym. Sci. Polym. Chem. Ed.,* **15,** 81 (1977).
20. J. P. Booth, G. Hancock, N. D. Perry, and M. J. Toogood, *J. Appl. Phys.,* **66,** 5251 (1989).
21. P. D. Richard, R. J. Mackunas, G. Lucovsky, G. G. Fountain, A. N. Mansow, and D. V. Tsu, *J. Vac. Sci. Technol. A,* **3,** 867 (1985).
22. C. R. Savage, R. B. Timmons, and J. W. Lin, *Chem. Mater.,* **3,** 575 (1991).
23. P. Jiang, D. J. Economou, and C. B. Shin, *Plasma Chem. Plasma Process.,* **15,** 383 (1995).
24. S. Samukawa, *Appl. Phys. Lett.,* **64,** 3398 (1994).
25. R. J. Gambogi, D. L. Cho, H. Yasuda, and F. D. Blum, *J. Polym. Sci. Part A Polym. Chem.,* **29,** 1801 (1991).
26. I. Sugimoto, *Macromolecules,* **24,** 1480 (1991).
27. C. R. Brundle, J. Evans, and S. Wilson, Eds., Encyclopedia of Materials Characterization, Butterworth-Heinemann, Boston, 1992.

28. M. B. Knickelbein, D. A. Webb, and E. R. Grant, *Mater. Res. Soc. Symp. Proc.,* **38,** 23 (1985).
29. S. J. Limb, C. B. Labelle, K. K. Gleason, D. J. Edell, and E. F. Gleason, *Appl. Phys. Lett.,* **68,** 2810 (1996).
30. F. W. Billmeyer, *J. Appl. Phys.,* **18,** 431 (1947).
31. W. Groh and A. Zimmermann, *Macromolecules,* **24,** 6660 (1991).
32. R. K. Wells, M. E. Ryan, and J. P. S. Badyal, *J. Phys. Chem.,* **97,** 12879 (1993).
33. D. R. Wheeler and S. V. Pepper, *J. Vac. Sci. Technol.,* **20,** 226 (1982).
34. D. T. Clark and W. J. Brennan, *J. Elect. Spectrosc. Rel. Phenon.,* **41,** 399 (1986).
35. R. d'Agostino, F. Cramarossa, and F. Illuzzi, *J. Appl. Phys.,* **61,** 2754 (1987).
36. A. Kono, M. Haverlag, G. M. W. Kroesen, and F. J. D. Hoog, *J. Appl. Phys.,* **70,** 2939 (1991).
37. S. G. Hansen, G. Luckman, and S. D. Colson, *Appl. Phys. Lett.,* **53,** 1588 (1988).
38. I. C. Plumb and K. R. Ryan, *Plasma Chem. Plasma Process.,* **6,** 205 (1986).
39. L. D. B. Kiss and H. H. Sawin, *Plasma Chem. Plasma Process.,* **12,** 523 (1992).